

# Coupled-Channel Enhanced SSFM for Digital Backpropagation in WDM Systems

S. Civelli<sup>1,2\*</sup>, E. Forestieri<sup>1,2</sup>, A. Lotsmanov<sup>3</sup>, D. Razdoburdin<sup>3,4</sup>, M. Secondini<sup>1,2</sup>

<sup>1</sup> TeCIP Institute, Scuola Superiore Sant'Anna, Via G. Moruzzi 1, 56124, Pisa, Italy

<sup>2</sup> PNTLab, CNIT, Via G. Moruzzi 1, 56124, Pisa, Italy

<sup>3</sup> Moscow Research Center, Huawei Technologies Co., Ltd., Moscow, Russia

<sup>4</sup> Sternberg Astronomical Institute, Moscow M.V. Lomonosov State University, Moscow, Russia

\*stella.civelli@santannapisa.it

**Abstract:** A novel technique for digital backpropagation (DBP) in wavelength-division multiplexing systems is introduced and shown, by simulations, to outperform existing DBP techniques for approximately the same complexity. © 2021 The Author(s)  
**OCIS codes:** 060.2330, 060.1660, 060.4510

## 1. Introduction

Digital backpropagation (DBP) is widely investigated for the mitigation of nonlinearity in optical fiber communication, with the split step Fourier method (SSFM) being the most popular method to practically implement DBP [1, 2]. The SSFM digitally inverts the optical channel by applying a number of steps in which linear and nonlinear effects are considered separately. Several alternative DBP techniques have been proposed to achieve the same performance as the SSFM with less steps and, hence, lower complexity, such as the correlated or filtered DBP [3, 4] and the enhanced SSFM (ESSFM) [5, 6].

While both the ESSFM and the classical SSFM are conceived for the propagation of a single channel, they can also be used for several wavelength-division multiplexing (WDM) channels, as long as they are jointly represented as a single optical field—we refer to this as *full-field* DBP. The potential gain achievable by full-field DBP increases with the number of jointly backpropagated channels [7]. However, the extremely large number of steps required in this case makes the practical implementation of full-field DBP not feasible [8].

In this work, we propose a novel technique for DBP—the *coupled-channel* ESSFM (CC-ESSFM)—which improves the ESSFM by explicitly accounting for the cross phase modulation (XPM) generated by several co-propagating channels and for its interplay with dispersion. We show, through simulations, that the CC-ESSFM achieves better performance than single- and full-field SSFM and ESSFM techniques for the same complexity.

## 2. Coupled-channel enhanced SSFM

The CC-ESSFM is described below for  $N_{ch}$  copropagating channels. The CC-ESSFM, like the SSFM and the ESSFM, consists of several steps  $N_s$ , made of a linear and a nonlinear part, and is depicted in Fig. 1(a).

In the linear part, the various channels are independently processed as in the SSFM or ESSFM, with the only difference that a time delay is introduced to account for the different group velocity of the channels and ensure that their contributions are correctly synchronized at each nonlinear step.

In the nonlinear part, a nonlinear phase rotation is applied to each polarization component of each channel to account for the self-phase modulation (SPM) and part of the XPM. According to the frequency-resolved logarithmic perturbation (FRLP) model [9], each channel induces a frequency-dependent nonlinear phase rotation which can be expressed as a quadratic form of its samples and affects the channel itself (SPM) and the other channels (XPM). The ESSFM accounts only for the SPM contribution and approximates it by a filtered version of the signal intensity, where the filter coefficients are numerically optimized to minimize the error [5, 6]. In the CC-ESSFM, on the other hand, also the XPM contributions are accounted for and expressed as filtered versions of the corresponding signal intensities. By assuming that each channel is separately represented over its bandwidth with  $n$  samples per symbol, the nonlinear step for the  $i$ th channel can be expressed as  $x'_i[k] = x_i[k] \exp(j\theta_i^x[k])$  and  $y'_i[k] = y_i[k] \exp(j\theta_i^y[k])$ , where  $x_i[k]$  and  $y_i[k]$  (and  $x'_i[k]$  and  $y'_i[k]$ ) are the  $k$ th samples of the two polarization components of the  $i$ th channel at the input (and output) of the nonlinear step, normalized to have unit power;

$$\theta_i^x[k] = - \sum_{\ell=1}^{N_{ch}} \left( \bar{\phi}_{i\ell}^{\parallel} \sum_{m=-N_c}^{N_c} C_{\ell-i}[m] |x_{\ell}[k+m]|^2 + \bar{\phi}_{i\ell}^{\perp} \sum_{m=-N_c}^{N_c} C_{\ell-i}[m] |y_{\ell}[k+m]|^2 \right) \quad (1)$$

$$\theta_i^y[k] = - \sum_{\ell=1}^{N_{ch}} \left( \bar{\phi}_{i\ell}^{\perp} \sum_{m=-N_c}^{N_c} C_{\ell-i}[m] |x_{\ell}[k+m]|^2 + \bar{\phi}_{i\ell}^{\parallel} \sum_{m=-N_c}^{N_c} C_{\ell-i}[m] |y_{\ell}[k+m]|^2 \right) \quad (2)$$

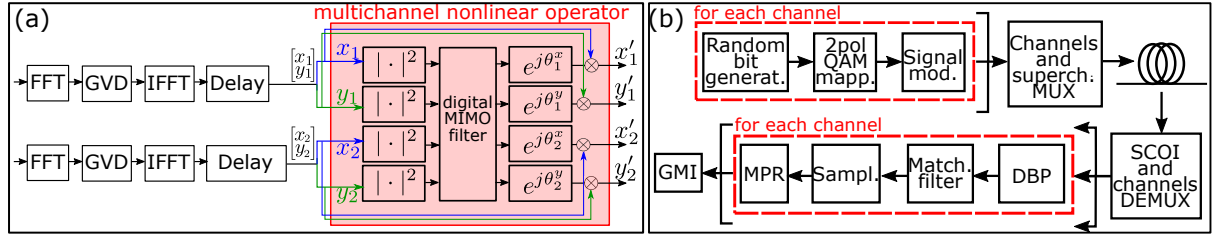


Figure 1. (a) Linear and nonlinear step of the CC-ESSFM for  $N_{\text{ch}} = 2$  channels. (b) System setup

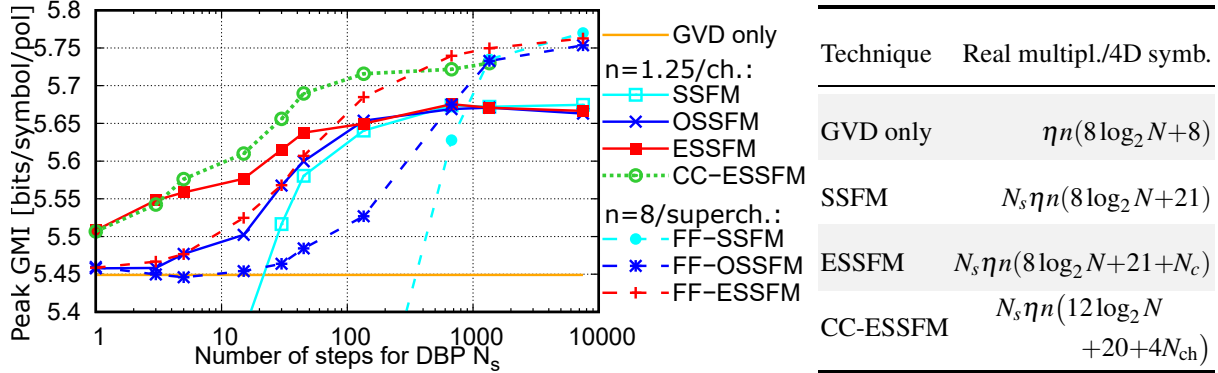


Figure 2. Performance of different DBP techniques versus number of steps  $N_s$ .

Table 1. Number of real multiplications per 4D symbol per channel.

are the (different) nonlinear phase rotations over the two polarization components;  $\bar{\phi}_\ell^\perp = \gamma P_\ell \int_{z-L/2}^{z+L/2} g(z) dz$  and  $\bar{\phi}_{i\ell}^\parallel = (2 - \delta_{i\ell}) \bar{\phi}_\ell^\perp$  are the average nonlinear phase rotations induced, respectively, by the copolarized and orthogonal component of the  $\ell$ th channel over the  $i$ th channel;  $\delta_{i\ell}$  is the Kronecker delta ( $\delta_{i,\ell} = 1$  if  $i = \ell$  and  $\delta_{i,\ell} = 0$  otherwise);  $P_\ell(z)$  is the power profile of the  $\ell$ th channel along the step of length  $L$ ;  $\gamma$  is the nonlinear coefficient; and  $C_{h=\ell-i}[m]$ , with  $m = -N_c, \dots, N_c$ , are the  $2N_c + 1$  real ESSFM coefficients which account for the effect of dispersion on the XPM generated by the  $\ell$ th channel over the  $i$ th channel.

With respect to the standard SSFM, the CC-ESSFM requires, at each step, the implementation of a digital  $2N_{\text{ch}} \times 2N_{\text{ch}}$  multi-input multi-output (MIMO) filter for the computation of (1) and (2). This can be efficiently done in frequency domain by using a pair of real FFTs and the corresponding IFFTs per each channel, with an overall increase in complexity of less than 50% compared to the SSFM. On the other hand, the single-channel ESSFM—equivalent to the CC-ESSFM with  $N_{\text{ch}} = 1$ —is more efficiently implemented in time-domain when the number of coefficients  $N_c$  is not too large. Table 1 reports the complexity of the ESSFM and CC-ESSFM compared to the standard SSFM and a simple dispersion compensation, considering the same implementation assumptions as in [6] and an overlap-and-save processing, where  $N$  is the “overlapping” block length and  $\eta$  the ratio between  $N$  and the actual number of samples “saved” per each processed block.

The CC-ESSFM coefficients can be obtained either by numerical optimization or analytically. In this work, we have adopted the numerical optimization, which guarantees a good performance and does not require the a priori knowledge of the link parameters, deferring the study of the analytical computation based on the FRLP model [9] to a future work. The numerical optimization is performed by assuming that the coefficients are independent of the launch power and satisfy the symmetry condition  $C_h[m] = C_{-h}[-m]$ , as predicted by the FRLP model and verified by numerical simulations. To further simplify the optimization, the coefficients  $\mathbf{C}_h = (C_h[-N_c], \dots, C_h[N_c])$  are obtained iteratively for  $h = 0, \dots, N_{\text{ch}} - 1$ , assuming  $N_c = 32$  for  $h = 0$  and  $N_c = 128$  for  $h > 0$ . At the  $h$ th iteration,  $\mathbf{C}_h$  is obtained by minimizing the mean square error over the received symbols, while keeping  $\mathbf{C}_0, \dots, \mathbf{C}_{h-1}$  fixed to the values found at the previous iterations, and setting  $\mathbf{C}_{h+1}, \dots, \mathbf{C}_{N_{\text{ch}}-1}$  to zero.

### 3. System setup and performance

The simulation setup is sketched in Fig. 1(b). The superchannel of interest (SCOI) is made of  $N_{\text{ch}} = 4$  channels with baud rate  $R_s = 41.67$  GBd, 75 GHz spacing, 64 quadrature amplitude modulation (QAM), and a root-raised-cosine pulse-shaping filter with a roll-off of 0.1. Two side superchannels with the same characteristics of the SCOI are included in the simulations. The link is made of 15 spans of 80 km single mode fiber (SMF) ( $D = 17$  ps/nm/km,  $\gamma = 1.3$ /W/km,  $\alpha_{\text{dB}} = 0.2$  dB/km); after each span, an erbium-doped fiber amplifier (EDFA) with a noise figure of 5 dB compensates for the loss. At the receiver side, after SCOI and channels demultiplexing, each channel of

the SCOI undergoes DBP—separately, or jointly when CC-ESSFM is employed—, matched filtering, and symbol-time sampling. On the other hand, when full-field DBP is used, it is performed over the entire SCOI, before channel demultiplexing. Finally, after removing a possible residual mean phase rotation (MPR) caused by nonlinearity and not compensated for by DBP, the average generalized mutual information (GMI) over the 4 channels of the SCOI is evaluated [10]. The number of samples per symbols considered for DBP is  $n = 1.25$  (per channel) for single-field and coupled-channel DBP, and  $n = 8$  (per superchannel) for full-field DBP. The optimization of the coefficients and the evaluation of the GMI are performed using a stream of 1024 and 65536 symbols per channel, respectively.

Figure 2 compares the peak GMI obtained at optimal launch power with different DBP techniques as a function of the number of steps  $N_s$ . For a small (but practical) number of steps, the conventional SSFM has a very poor performance—in fact, even worse than simple GVD compensation. In this case, the performance can be improved (without changing the complexity) by using the optimized SSFM (OSSFM), with a numerically optimized nonlinear coefficient (lower than the actual one) in the nonlinear step [8]. An even better performance is achieved by the ESSFM, while the best performance is achieved by the CC-ESSFM. In this practical scenario, the full-field techniques (dashed lines) perform significantly worse than the corresponding single-channel ones (solid lines), due to the larger accumulated dispersion in each step. The picture changes when the number of steps is increased to less realistic values. In this case, the full-field techniques outperform the corresponding single-channel techniques and perform even slightly better than the CC-ESSFM. Asymptotically ( $N_s \rightarrow \infty$ ), all the single-channel techniques converge to the same limit, corresponding to an exact compensation of intrachannel effects. Analogously, all the full-field techniques converge to a higher limit, corresponding to an exact compensation of intra-superchannel effects, while CC-ESSFM converges to a slightly lower limit, as it accounts only for SPM and XPM in the SCOI.

Though the number of steps is a good indicator of the relative complexity of the various algorithms, the actual complexity depends on the specific algorithm and on the details of the implementation. Table 1, obtained under some reasonable but simplifying assumptions, allows a more accurate comparison and shows that ESSFM and CC-ESSFM require, respectively, about 30% and 50% more multiplications per step than SSFM, hence only slightly reducing their advantage compared to the other techniques in Fig. 2. However, we believe that additional simplifications and a careful implementation can further reduce these figures.

Similar results (not shown here for lack of space) have been obtained when considering probabilistically-shaped QAM modulations and when including a practical carrier phase recovery algorithm at the receiver.

#### 4. Conclusion

We have proposed the CC-ESSFM as an efficient technique for multi-channel DBP in WDM systems. By additionally accounting for XPM among the channels and its interplay with dispersion, the CC-ESSFM outperforms conventional single-channel and full-field DBP techniques for the same (sufficiently small) number of steps.

#### References

1. R. J. Essiambre and P. J. Winzer, “Fibre nonlinearities in electronically pre-distorted transmission,” in *Proc. Eur. Conf. Opt. Commun. (ECOC)*, , vol. 2 (2005), pp. 191–192.
2. E. Ip and J. M. Kahn, “Compensation of dispersion and nonlinear impairments using digital backpropagation,” *J. Light. Technol.* **26**, 3416–3425 (2008).
3. L. Li, Z. Tao, L. Dou, W. Yan, S. Oda, T. Tanimura, T. Hoshida, and J. C. Rasmussen, “Implementation efficient nonlinear equalizer based on correlated digital backpropagation,” in *Opt. Fiber Commun. Conf. (OFC)*, (2011), p. OWW3.
4. D. Rafique, M. Mussolin, M. Forzati, J. Mårtensson, M. N. Chughtai, and A. D. Ellis, “Compensation of intra-channel nonlinear fibre impairments using simplified digital back-propagation algorithm,” *Opt. Express* **19**, 9453–9460 (2011).
5. M. Secondini, D. Marsella, and E. Forestieri, “Enhanced split-step Fourier method for digital backpropagation,” in *2014 The European Conference on Optical Communication (ECOC)*, (IEEE, 2014), pp. 1–3.
6. M. Secondini, S. Rommel, G. Meloni, F. Fresi, E. Forestieri, and L. Poti, “Single-step digital backpropagation for nonlinearity mitigation,” *Photon. Netw. Commun.* **31**, 493–502 (2016).
7. R. Dar and P. J. Winzer, “Nonlinear interference mitigation: methods and potential gain,” *J. Light. Technol.* **35**, 903–930 (2017).
8. G. Liga, T. Xu, A. Alvarado, R. I. Killey, and P. Bayvel, “On the performance of multichannel digital backpropagation in high-capacity long-haul optical transmission,” *Opt. Express* **22**, 30053–30062 (2014).
9. M. Secondini, E. Forestieri, and G. Prati, “Achievable information rate in nonlinear WDM fiber-optic systems with arbitrary modulation formats and dispersion maps,” *J. Light. Technol.* **31**, 3839–3852 (2013).
10. A. Alvarado, E. Agrell, D. Lavery, R. Maher, and P. Bayvel, “Replacing the soft-decision FEC limit paradigm in the design of optical communication systems,” *J. Light. Technol.* **33**, 4338–4352 (2015).